

# Diffusion in the aged aluminium film on iron\*

A Y Galashev<sup>†</sup>, O R Rakhmanova, V A Kovrov, and Yu P Zaikov

*Institute of High-Temperature Electrochemistry, Ural Branch of Russian Academy of Sciences, Yekaterinburg 620990, Russia*

(Received 24 October 2016; revised manuscript received 30 November 2016; published online 13 February 2017)

Metallic coatings of many types can be applied to steel to provide outstanding, long-term corrosion protection. A thin Al film is studied at an Fe substrate by the molecular dynamics method at temperatures ranging from 300 K to 1173 K. Al atoms are found to penetrate the Fe matrix at a temperature of 873 K. The potential energy of the system changes step-like at a temperature of 1173 K. At such temperature mean square atomic displacement significantly changes. The behaviors of the Al and Fe diffusion coefficients are mainly determined by the temperature dependence of the diffusion activation energy.

**Keywords:** aluminium film, diffusion coefficients, iron, molecular dynamics

**PACS:** 82.20.Wt, 81.15.Aa

**DOI:** 10.1088/1674-1056/26/3/038201

## 1. Introduction

Steel is prone to rusting, and thus its surface becomes unsightly. For this reason, steel is protected by a variety of methods including metallic coatings. Corrosion is an electrochemical process that, in the case of steel, oxidizes the iron in the steel and causes it to become thinner over time. Oxidation (or rusting) occurs as a result of the chemical reaction between steel and oxygen. In the case of most low-carbon steel products, iron oxide (rust) develops on the surface and is not protective because it does not form a continuous, adherent film. Metallic coatings can be applied to steel in a very cost-effective manner to furnish the sufficient corrosion protection. Metallic coatings protect steel in two principal ways. Firstly, like paint, they provide barrier protection, and secondly, they give galvanic protection in most instances. Aluminum provides good barrier protection for steel sheets. Like steel and zinc, aluminum reacts in air to form an oxide film on its surface. However, in contrast to the behavior of iron oxide, and similar to what happens with zinc, the aluminum oxide film stays intact. The  $\text{Al}_2\text{O}_3$  layer acts as a very tightly adhering film on the surface of aluminum. By preventing fresh aluminum from exposing to air and moisture, this intact film stops further corrosion of the underlying aluminum. The oxide behaves as a stable non-corroding film, rendering the surface passive in most environments. In total, metallic coatings such as Al can be applied to steel very cost-effectively to provide outstanding, long-term corrosion.

Al, as with the majority of other metals, is not corrosion-resistant according to a number of reasons: humidity may remain within the substrate, bad welding or incorrect contact with other metals. Al–Mg and Al–Mn alloys demonstrate good corrosion resistance. Extra pure Al (> 99.9% Al) has the best anticorrosion properties. The corrosion resistance proper-

ties of alloys abruptly decrease when other metals, especially Cu and Fe, are added. Al protective coatings are applied in different ways on steel, cast iron, copper, titan and brass. For instance, in the alitizing process, when steel is placed into liquid Al, diffusion processes result in the formation of solid Al–Fe compounds at the surface of steel. Near the liquidus temperatures of Al–Fe alloys (3.5–10 at% of Fe) the  $\text{Al}_3\text{Fe}$  crystal sedimentation and their following melting were observed.<sup>[1]</sup> A chemical compound of two or more metals (intermetallide) has a set ratio between the components.

Intermetallic compounds are of great interest due to their high-temperature strengths, low densities, and high creep resistance.<sup>[2,3]</sup> However, intermetallides are not widely used because of their brittleness at room temperature.<sup>[4]</sup> The addition of plastic metallic phase into intermetallide provides a good combination of strength and impact resistance. Properties of such compounds are functions of intermetallic layer thickness, structure, and sequential location in high-strength matrix. There is a reactive diffusion between the alternately placed layers of two different metals. The intermetallide layer at the interface grows during annealing. To optimize such properties as impact resistance and strength, it is vital to understand the diffusion process kinetics. Nowadays there is a lack of data on solid body diffusion in the Al–Fe system.

Properties of a solid material and mainly its structure are determined by the liquid alloy solidifying process. For instance, properties of light Al-based alloys change, depending on the casting temperature condition.<sup>[5]</sup> The diffusion coefficient  $D$  is important for understanding the solidifying processes, including crystal growth<sup>[6]</sup> and glass formation.<sup>[7]</sup> The diffusion coefficient  $D$  of even liquid Al is hard to detect experimentally. The capillary tube method is usually used to measure directly the diffusion coefficients in liquid alloys. This

\*Project supported by the Ministry of Science and Education of the Russian Federation (Grant No. 14.607.21.0035, unique identifier RFMEFI60714X0035).

<sup>†</sup>Corresponding author. E-mail: alexander-galashev@yandex.ru

© 2017 Chinese Physical Society and IOP Publishing Ltd

<http://iopscience.iop.org/cpb> <http://cpb.iphy.ac.cn>

method requires an isotope to be used as an indicator. The effect of a convective flow existing along the profile of diffusion during annealing may lead to severe overestimation of value  $D$ . In addition, no radioactive isotope is available for aluminum. The present work is aimed to study the diffusion process with Al contacting Fe, to analyze the temperature influence on the process and to evaluate Al protective properties for steel construction.

## 2. Computer model

Al and Fe cubic cells vertically located one on another with a contacting face (100) serve as an original simulation configuration. In addition, the minimum distance between Al and Fe atoms is equal to an average distance between the atoms in Al and Fe crystals. The top cell contains 864 Al atoms, packed into a face-centered cubic lattice. The bottom cell contains 1024 Fe atoms which occupy sites in a body-centered cubic lattice. The calculations are carried out in parallel for 5 temperature values in a range of 300–1173 K. The equations of motion are integrated by the fourth-order Runge–Kutta method in time steps of  $\Delta t = 10^{-16}$  s.

Aluminum is characterized by superb corrosion resistance and applicability, high thermal and electrical conductivities but low mechanical properties. Aged aluminum has relatively poor fatigue properties compared with the other metals due to metastable structure under cyclic stresses. We aim to determine the self-diffusion coefficient in an aluminum coating exposed to strong periodic stress during operation. In this case, the artificial aging of the material may be performed by using cyclic loads. Maximum cyclic loading  $\sigma_{zz}^0$  in the axial direction achieves 300 MPa. Actually, the experimental axial elastic limit observed in Ref. [8] is  $\sim 210$  MPa, while the equivalent shearing one is only  $\sim 140$  MPa. In this work the external axial load is in the following form:

$$\sigma_{zz} = \sigma_{zz}^0 \sin(\omega t), \quad (1)$$

with the period of 1 ps. We use 10 load cycles of constant amplitude. Cyclic stress in the aluminum film is produced by applying a periodic force field  $f_z$ . The procedure for creating the external cyclic load is disconnected after 10 ps and the calculation continues. Here we do not consider the formation nor the structure of cracks in detail because our aim is to study the behaviors of aged aluminum film on iron at low and high temperatures.

The Al crystal is found to crack, the upper part of the crystal almost separates from the thin crystalline Al film, which remains at the Fe substrate, at the temperatures of  $T \leq 873$  K. The brittle Al crystal cracks because Al atoms are pulled by Fe atoms, the differences in interatomic distance and asynchronous vibrations of atoms in different subsystems. Then

the separated upper part of the Al crystal is removed from each system. From 127 (300 K) to 144 (873 K) Al atoms remain at the Fe substrate. A new calculation launched after the upper Al crystal part removal lasts  $10^7$  time steps (1 ns) at each temperature. No visible separation of the Al crystal is observed at the temperature of 1173 K after calculating under the cyclic load during 10 ps. The calculations at this temperature are performed for the whole system comprised of 1888 atoms (864 Al + 1024 Fe), the calculations length is 2 ns. In all cases the periodic boundary conditions (PBC) function only horizontally. The highest and the lowest system boundaries have free boundary conditions.

The Finnis–Sinclair (the generalized EAM) potential is used to describe Al–Al, Fe–Fe, and Al–Fe interactions.<sup>[9]</sup> It is justified from the viewpoint of electron theory of solid body. The total energy of an atom  $i$  is given by

$$U_i = F_\alpha \left( \sum_{j \neq i} \rho_{\alpha\beta}(r_{ij}) \right) + \frac{1}{2} \sum_{j \neq i} \phi_{\alpha\beta}(r_{ij}), \quad (2)$$

where  $F$  is the embedding energy which is a function of the atomic electron density  $\rho$ ,  $\rho$  is a function specific to the atomic types of both atoms  $i$  and  $j$ , so that different elements can contribute differently to the total electron density;  $\phi$  is a pair potential interaction;  $\alpha$  and  $\beta$  are the element types of atoms  $i$  and  $j$ , respectively. The multi-body nature of the Finnis–Sinclair potential is a result of the embedding energy term. This potential takes into account the temperature effects automatically because  $\rho$  is a function of temperature according to definition. Potential parameters for Al–Fe system are taken from Ref. [9].

A simplified model of the diffusion of atoms in any crystal is as follows: at low temperatures an atom moves according to a common diffusion–vacancy mechanism, whereas at high temperatures a collective diffusion is possible.<sup>[10]</sup> The difference in energy  $E_a = E^* - E_0$  between the initial state of the atom  $E_0$  and its energy in the saddle point  $E^*$  is defined as the activation energy of moving atom. Usually the basic state is considered to be that at a zero temperature, in crystal it is the node of ideal crystalline lattice. The value  $E_a$  is determined as a difference between the maximum and minimum potential energies of the whole system in the case where an atom moves from one interstitial site to another. The energy  $E^*$  has a stochastic nature. A diffusion coefficient of the atom in crystal may be presented in the following form:<sup>[11]</sup>

$$D = D_0 \exp \left( -\frac{E_a}{kT} \right), \quad (3)$$

where  $D_0$  is the constant independent of temperature  $T$  and  $k$  is the Boltzmann constant.

The energy  $E_a$  may be defined according to

$$E_a = \bar{E} + E_f - E_0, \quad (4)$$

where  $\bar{E}$  is the average system energy at temperature  $T$ ,  $E_f$  is the energy fluctuation swing, and  $E_0$  is the energy of this system at  $T = 0$  K.

In liquid or gas medium, the coefficient  $D$  is calculated according to the change of atom location in three-dimensional spatial coordinates by using the following Einstein's equation:

$$D = \lim_{t \rightarrow \infty} \frac{1}{6t} \left\langle \frac{1}{N} \sum_{i=1}^N [r_i(t) - r_i(t_0)]^2 \right\rangle, \quad (5)$$

where  $r_i$  is the radius vector of the atom  $i$  and the angle brackets denote averaging over the initial time  $t_0$ .

The diffusion barrier for carbon atoms in Fe, for example, in a temperature range of 600–800 K is 0.77–0.90 eV (molecular dynamic (MD) calculation), which is in agreement with the calculation by using the density functional theory (0.86 eV).<sup>[12]</sup> At 400 K,  $D$  is equal to  $4.47 \times 10^{-17}$  m<sup>2</sup>/s according to MD calculations.<sup>[13]</sup>

For a detailed analysis of the structure of the Fe subsystem, the method of statistical geometry is employed. Voronoi polyhedron (VP) is constructed for each from 500 atoms of Fe placed closest to the center of mass of the MD cell. Constructing these polyhedra is possible in the least-populated half space where at least one atom exists. The polyhedra are defined by atom coordinates written in every 10000 time steps. In total, 500000 polyhedra are constructed.

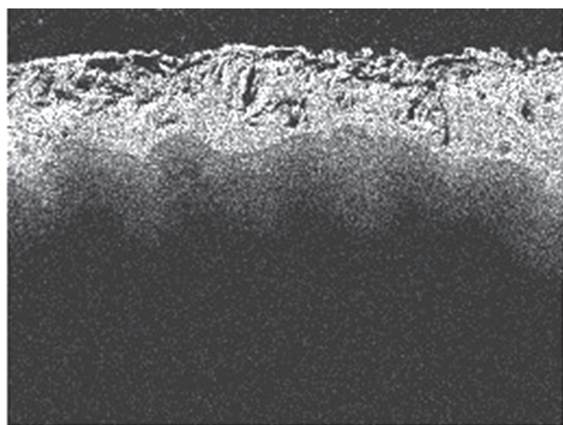


**Fig. 1.** General view of the Al film (light image) on the steel rod (dark part at the bottom) obtained by the electrolytic alitizing and annealing.

A steel electrode requires the Al coating for protecting the aggressive environment which causes Fe to corrode. Alitizing and electrolytic alitizing are general methods used to coat Fe with the Al film. Irrespective of the Al film formation technique, the pre-Fe surface should be cleaned off the oxide film. The annealing is performed to strengthen the Al film coating on the steel construction. This results in the interdiffusion of metal atoms, thereby forming a diffusion layer and an intermetallide layer. Figure 1 demonstrates the Al film on a steel rod. The image is obtained by using the NEOFOT 32 microscope. The coating is formed by the electrolysis at  $T = 1193$  K

with the following annealing.<sup>[14]</sup> Al (light spot in Fig. 1) in the form of separate dendrites penetrates Fe lattice, and Fe penetrates inside the Al coating (dark blotches and darkening the Al surface, facing the Fe substrate). Through such a joint, the Al film is firmly fixed on the Fe substrate. The Al melting point ( $T_m^{\text{Al}} = 933$  K) is much lower than that of Fe ( $T_m^{\text{Fe}} = 1808$  K). Calculations are performed by using the hybrid computer cluster “URAN” (Institute of Math and Mechanics UB RAS) with a peak capacity of 216 Tflop/s and 1864 CPU.

### 3. Results

Figure 2 illustrates the “Al film at Fe substrate” system configuration after  $10^7$  time steps obtained for the temperatures of 300 K and 873 K. Al film at Fe substrate has a crystalline structure at 300 K. However, there are sites occupied by Fe atoms in the Al atoms rows.

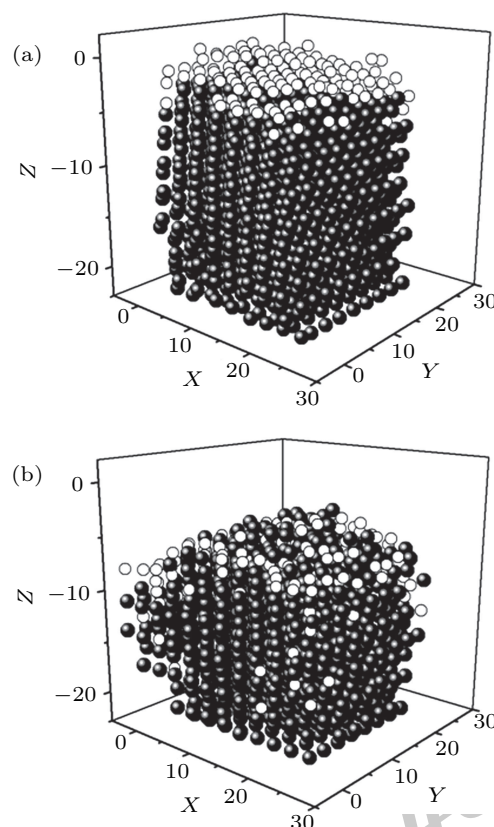


**Fig. 2.** “Al film at Fe substrate” system configurations obtained at the time moment of 1 ns and temperatures: (a) 300 K and (b) 873 K. The atoms coordinates are presented in angstroms.

Sometimes Fe atoms integrate into the Al lattice in the form of quite long non-linear chains. The Al atoms penetrate the Fe lattice mostly at short distances. But along the crystal edges and some faces of the MD cell the Al atoms penetrate into Fe much farther up to two interatomic distances. At 873 K the Al atoms do not totally occupy the top face of the MD cell and the film has an irregular structure. Only separate regions with locally ordered structures remain. A top plan view

demonstrates the presence of twisted chains and cyclic formations from the Al atoms. Single Fe atoms and Fe atom groups appear at the Al film surface. There is a surface melting of the iron where clusters of Fe atoms and sparse areas are observed. The top face of the MD cell has a convex form. Some individual Al atoms move along the faces of the MD cell at distances comparable to its edge.

The temperature dependence  $U_{\text{tot}}(T)$  of Al film at Fe substrate system potential energy is illustrated in Fig. 3. The monotonic increase of the energy  $U_{\text{tot}}$  is seen until  $T = 873$  K. The  $U_{\text{tot}}$  energy increases sharply in a range between 873 K and 1173 K. Such a behavior of the  $U_{\text{tot}}(T)$  function justifies the presence of phase transition in the system. A dashed line in Fig. 3 denotes the asymptotic extension of the  $U_{\text{tot}}(T)$  function to the low-temperature region. The point of contact between the function extension and the  $Y$  axis provides the  $U_0$  value, which corresponds to the value of potential energy  $U_{\text{tot}}$  at absolute zero. The temperature difference  $U_{\text{tot}} - U_0$  is defined as the activation energy of the defect formation in Fe matrix and Al crystalline film. The inset shows the time change in energy  $U_{\text{tot}}$  at  $T = 300$  K. It is seen that the equilibrium of the system is reached at the time moment of 0.4 ns.

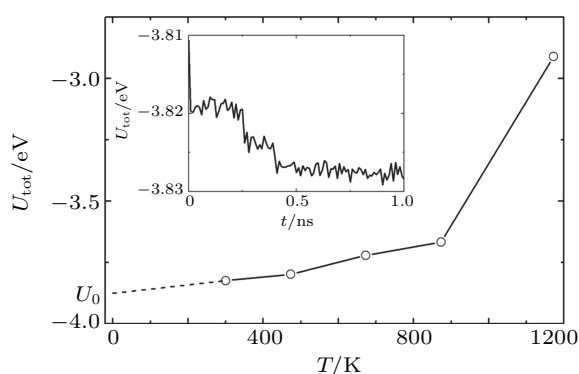


**Fig. 3.** Temperature dependence of the “Al film at Fe substrate” system potential energy. Dashed line denotes a linear approximation of the  $U_{\text{tot}}(T)$  function to  $T = 0$  K. The insertion presents the time change in the system potential energy at  $T = 300$  K.

The Fe substrate structure in the transition region  $\alpha \rightarrow \gamma$  is studied using the static geometry method. Figure 4(a) presents angular distributions ( $\theta$ -distributions) of nearest geometric neighbors of the Fe-subsystem at 873 K and 1173 K. The angles  $\theta$  formed by a pair of the nearest geometric neighbors with the central particle, that is, the particle around whose center a VP is constructed, are distributed in the interval  $[0, 180^\circ]$ . We consider the absolute values of these angles. The locations of three main peaks (at  $60^\circ$ ,  $72^\circ$ , and  $126^\circ$ ) of the  $\theta$ -distribution at  $T = 873$  K are in good agreement with the positions of basic peaks in analogous distribution for a body-centered cubic crystal.<sup>[15]</sup> At the same time a wide domed-shape angular distribution at  $T = 1173$  K corresponds to the analogous  $\theta$ -distribution for a disordered lattice,

which was obtained at the two-component face-centered crystal destruction.<sup>[16]</sup> The distribution of faces on the number of edges,  $m$ , is provided in Fig. 4(b). At 873 K tetragonal faces dominate in  $m$ -spectrum of the Fe subsystem, i.e., the system has symmetry of order 4. At 1173 K a wide  $m$ -distribution is obtained for this system, i.e., 5- and 6-edged faces are the most frequently observed. To specify the predominant structure type (regular or irregular) at 1173 K the heat noise is filtered at the statistic-geometry analysis. Small-scale thermal fluctuations in the VP are prevented by eliminating the edges each with a length of  $l < 0.5\bar{l}$ , where  $\bar{l}$  is an average size of the VP edge length. This procedure is usually accompanied by the exclusion of small faces in the VP. The insert in Fig. 4(b) demonstrates the Fe subsystem  $m$ -distribution after eliminating small edges. The tetragonal faces are seen to dominate for such a distribution, i.e., there is a large possibility of a crystalline phase formation in the Fe subsystem.

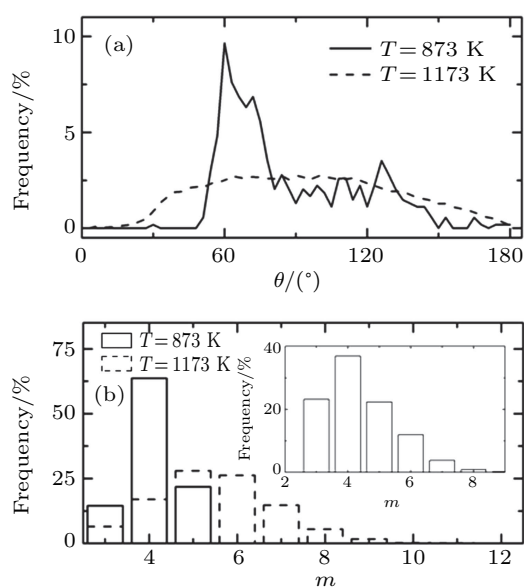


**Fig. 4.** Angular distribution of nearest geometric neighbors, and (b) distribution of faces on the number of the polyhedron sides in Fe subsystem at temperatures of 873 K and 1173 K. The insert presents  $m$ -distribution of faces at 1173 K when edges each with a length of  $l < 0.5\bar{l}$  were excluded.

Figure 5 demonstrates the evolutions of the Al and Fe mean square displacements at 873 K and 1173 K. The  $\langle(\Delta r)^2\rangle(t)$  function represents a typical time dependence for a solid body at 873 K, i.e., the function has a growth region with a continuous decrease in the angle with respect to the time axis, which topples to a “plateau”. Further increasing temperature 1173 K leads to the formation of the  $\langle(\Delta r)^2\rangle(t)$  time dependence with an increasing inclination which eventually reaches a constant value. Such dependences usually characterize a non-equilibrium state of the system appearing during the phase transition but they can also describe a liquid state. The diffusion coefficient  $D$  values of Fe and Al atoms which are calculated according to the  $\langle(\Delta r)^2\rangle(t)$  inclination

to the time axis at 873 K and 1173 K are  $3.3 \times 10^{-13} \text{ m}^2/\text{s}$  and  $7.8 \times 10^{-13} \text{ m}^2/\text{s}$ , correspondingly. The analogous  $D$  determination at lower temperatures under consideration is associated with a large uncertainty due to the “plateau”.

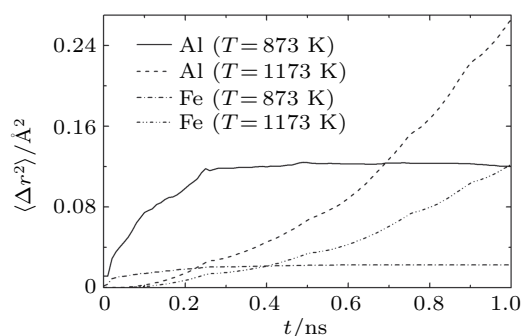


Fig. 5. Mean square atomic displacements of Al and Fe atoms at the temperatures of 873 K and 1173 K.

Due to a short observation period of the system during MD simulations as compared with that of the physical experiment, it appears impossible to trace a real diffusion (the movements of atoms in the lattice on the distances comparable to interatomic ones) in crystal even at high temperatures. It is possible to determine only a local atomic mobility at a desired temperature but not the diffusion coefficient. This is why a real diffusion for the metal crystal with long-range interactions should be described by considering the diffusion activation energy. It is impossible to study such a diffusion in a general MD crystal model. To describe the real diffusion we use the experimental value  $E_a$ . The radioactive Fe diffusion is measured for both monocrystals and polycrystalline Al samples at a temperature interval of  $793 \text{ K} \leq T \leq 933 \text{ K}$ .<sup>[17]</sup> The  $\log[D](T)$  dependence obtained for Fe in Al crystal is presented by curve III in Fig. 6. Curve IV in Fig. 6 shows the assessed values of  $\log[D]$  for Fe in Al foil in a temperature interval of  $773 \leq T \leq 873 \text{ K}$ .<sup>[18]</sup> One of our calculations ( $T = 873 \text{ K}$ ) is executed within the temperature interval studied in Ref. [16]. We adopt  $E_a = 0.8787 \text{ eV}$  and  $D = 3.07 \times 10^{-14} \text{ m}^2/\text{s}$  at  $T = 873 \text{ K}$ , and these values of diffusion coefficient and activation energy are given in Refs. [17] and [18], respectively. We determine the value of  $D_0$  according to relation (3). Then considering  $E_f$  to be a constant, the temperature corrections to the  $E_a$  value are found by using MD calculations:  $\Delta E_a = \bar{U}_{\text{tot}}(T) - \bar{U}_{\text{tot}}(873 \text{ K})$ . Curve I in Fig. 6 demonstrates the above described  $\log[D](T)$  dependence. Curve II illustrates the analogous dependence which is obtained at a constant value of the  $E_a$  activation energy corresponding to 873 K. Point 5 denotes the  $\log[D]$  value of Fe atoms at  $T = 1173 \text{ K}$  calculated by using MD simulation. The value is seen to be lower than that predicted by the curve I, but this value accords well with the value determined by the curve II. Note that there is close agreement between curve I and the

$\log[D](T)$  experimental dependence in the region of  $D$  determination in work.<sup>[17]</sup> Curves I and II closely pass through the temperature interval of  $\log[D]$  determined in Ref. [18]. The temperature dependence of the activation energy  $E_a$  strongly affects the  $\log[D]$  value, especially at  $T = 300 \text{ K}$ , where the difference between the values determined by using curves I and II is 10 orders of magnitude. Al atoms diffusion in Fe matrix is characterized by a diffusion coefficient approximately twice larger than that of Fe atoms in Al film according to the mass ratio  $m_{\text{Fe}}/m_{\text{Al}} \approx 2$ . According to the scheme of the diffusion process shown in Fig. 6 the graphics for Al and Fe coincide.

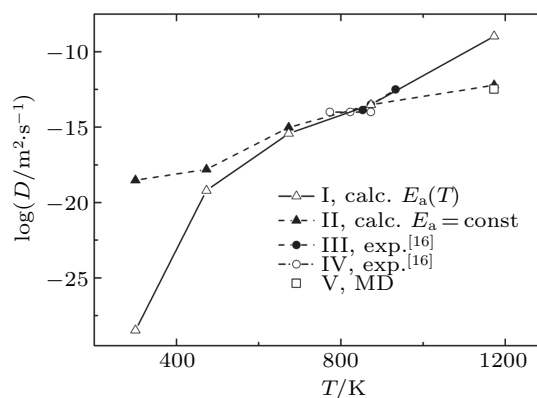


Fig. 6. Fe atoms diffusion in  $\log[D]-T$  coordinates.

#### 4. Discussion

The efficient fuel utilization requires a significant decrease in steel usage in the motor industry. Due to the fact that steel has a large relative density it is unusable in aviation. The creation of steel alloy with a light metal can solve the problem. Al as well as Fe (a basic steel component) is a widespread and cheap metal. However, the Fe–Al–C alloy is too brittle. The manganese addition significantly improves properties of aluminium steel but nevertheless it remains unusable in vehicle production.

The Al-based intermetallic phases  $\text{Fe}_3\text{Al}$  and  $\text{Ni}_3\text{Al}$  are referred to as structural materials and coatings for high-temperature applications. They demonstrate high corrosion resistance due to the formation of a dense aluminium oxide film. Aluminium oxide, especially  $\alpha\text{-Al}_2\text{O}_3$ , provides a low oxidation rate even at temperatures above  $1273 \text{ K}$ .<sup>[19]</sup> Unlike chromium, which is present in conventional stainless steels and alloys based on nickel, aluminium oxide does not evaporate above  $1273 \text{ K}$ . It is also stable in the oxygen-depleted atmosphere. Nickel–graphene and aluminium–graphene films have even higher thermal stability.<sup>[20,21]</sup>

The present study provides a complete outlook of the kinetic changes observed in the physical experiment.<sup>[18]</sup> The experiment<sup>[18]</sup> aimed at the following. The aluminum foil

sandwiched between two sheets of steel after a thorough cleaning of surfaces was rolled up at 773 K. The tied rolls were annealed at different temperatures for various times to synthesize Al-Fe intermetallide layer. Then the samples were placed into the epoxide resin and cut perpendicularly to the reaction surface, they were polished and analyzed under the optic microscope to determine the thickness values of Al, Fe and aluminide layers. The XRD image analyses distinctly demonstrate the presence of the  $\text{Fe}_2\text{Al}_5$  phase. It appears possible to control the aluminide phase growth. The activation energy of the  $\text{Fe}_2\text{Al}_5$  layer growth is 0.8787 eV. The calculated coefficient of Fe and Al interdiffusion through the  $\text{Fe}_2\text{Al}_5$  layer is of the order of  $10^{-14}$   $\text{m}^2/\text{s}$ .

The Einstein relation (5) does not permit calculation of the self-diffusion coefficient in the metal crystals in MD model with an adequate accuracy. We can judge this according to the form of curve 1 in Fig. 6. However, using experimental data it is possible to widen significantly the temperature interval in which the  $D$  value is determined for solid metal. Figure 6 illustrates that the diffusion activation energy has a determinative influence on  $D$  value. All in all the self-diffusion characters observed in the specimen under the microscope and calculated using MD simulation are identical. When Al is in a solid state, the diffusion of light Al atom into Fe matrix is more intensive; but when Al is completely molten (at  $T = 1173$  K), a large number of Fe atoms easily penetrate Al melt. Due to the fact that Fe remains solid at  $T = 1173$  K, the diffusion of the Fe atoms into the aluminum prevails over the diffusion of the Al in the iron.

## 5. Conclusions

The MD simulation is used to study the diffusion layer formation during the Al film heating at Fe substrate. The atomic diffusion of a lighter metal has a form of separate sharp "bursts", whereas Fe heavy atoms move into Al lattice in a wide wave-like front. This accords with the experimentally observed penetration of Al atoms into Fe substrate. A thin Al film, left at the Fe surface, almost all spreads out over the top and side surfaces of the MD cell at  $T = 873$  K. Part of

the Al atoms diffuses into the Fe matrix volume. Diffusing Fe atoms appear at the Al film surface in the form of chains and small islands. The potential energy of the whole system monotonically increases up to  $T = 873$  K. When the temperature reaches 1173 K the mean square displacements of Al and Fe atoms change their behavior from the typical characteristic of a solid state to that of a liquid one. The diffusion coefficients of Fe and Al atoms determined in the present work deviate from the parabolic dependence in the  $T$ - $\log[D]$  coordinates at high temperatures ( $T > 873$  K), which is probably due to the presence of structural transition in the Fe matrix at  $T = 1173$  K. At the temperatures of  $T < 1173$  K the diffusion of Fe atoms into the Al film is controlled by interatomic forces in Fe, keeping the Fe atoms localized in the cells formed by the nearest neighbors.

## References

- [1] Beltukov A L, Menshikova S G and Ladyanov V I 2015 *High Temp.* **53** 491
- [2] Zhang J P, Zhang Y Y, Wang E P, Tang C M, Cheng X L and Zhang Q H 2016 *Chin. Phys. B* **25** 36102
- [3] Ai L Q, Zhang X X, Chen M and Xiong D X 2016 *Acta Phys. Sin.* **65** 96501 (in Chinese)
- [4] Stoloff N S, Liu C T and Deevi S C 2000 *Intermetallics* **8** 1313
- [5] Jakse N and Pasture A 2013 *Sci. Rep.* **3** 3135
- [6] Kasperovich G, Meyer A and Ratke L 2010 *Int. Found. Res.* **62** 8
- [7] Inoue A 2000 *Acta Mater.* **48** 279
- [8] May A, Taleb L and Belouchrani M A 2013 *13th International Conference on Fracture* (Beijing, China) p. 1
- [9] Mendeleev M I and Srolovitz D J 2005 *J. Mater. Res.* **20** 208
- [10] Alekseenko V V 2008 *Phys. Solid State* **50** 1848
- [11] Novoselov I I, Kuksin A Yu and Yanilkin A V 2014 *Phys. Solid State* **56** 1025
- [12] Lau T T, Först C J, Lin X, Gale J D, Yip S and van Vliet K J 2007 *Phys. Rev. Lett.* **98** 2155011
- [13] Ishii A, Ogata S and Kimizuka H 2012 *Phys. Rev. B* **85** 064303
- [14] Zaikov Yu P, Kovrov V A, Brodova I V, Shtefanyuk Yu N, Pingin V K and Vinogradov D I 2015 *Adv. Mater. Res.* **1088** 250
- [15] Galashev A E and Mukhina I G 1992 *Phys. Met. Metallogr.* **74** 544
- [16] Galashev A E and Skripov V P 1986 *J. Struct. Chem.* **27** 407
- [17] Gao B, Nalano S and Kakimoto K 2011 *Cryst. Growth Des.* **12** 522
- [18] Jindal V, Srivastava V C, Das A and Ghosh R N 2006 *Mater. Lett.* **60** 1758
- [19] Klower J 1996 *Mater. & Corros* **47** 685
- [20] Galashev A E 2014 *High Temp.* **52** 633
- [21] Galashev A Ye and Rakhmanova O R 2014 *High Temp.* **52** 374

JUST FOR AUTHORS  
— CHINESE PHYSICS B